Am J Cancer Res 2023;13(10):4944-4960
www.ajcr.us /ISSN:2156-6976/ajcr0149386

Original Article

KIF15 knockdown inhibits colorectal cancer proliferation and migration through affecting the ubiquitination modification of NRAS

Debing Shi[1,2], Jianwei Wang[3], Qun Deng[3], Xiangxing Kong[3], Ying Dong[4], Yongzhi Yang[1], Ye Xu[1,2], Limian Ling[3], Yurong Jiao[3], Shaojun Yu[3]

[1]Department of Colorectal Surgery, Fudan University Shanghai Cancer Center, 270 Dong'an Road, Shanghai 200032, China; [2]Department of Oncology, Shanghai Medical College, Fudan University, 270 Dong'an Road, Shanghai 200032, China; [3]Department of Colorectal Surgery and Oncology, Key Laboratory of Cancer Prevention and Intervention, Ministry of Education, The Second Affiliated Hospital, Zhejiang University School of Medicine, 88th, Jiefang Road, Hangzhou 310000, Zhejiang, China; [4]Department of Medical Oncology, The Second Affiliated Hospital, Zhejiang University School of Medicine, 88th, Jiefang Road, Hangzhou 310000, Zhejiang, China

Received January 29, 2023; Accepted September 15, 2023; Epub October 15, 2023; Published October 30, 2023

Abstract: As one of the most common malignancies, colorectal cancer (CRC) requires a thorough understanding of the mechanisms that promote its development and the discovery of new therapeutic targets. In this study, immunohistochemical staining confirmed significantly higher expression levels of KIF15 in CRC. qPCR and western blot results demonstrated the effective suppression of KIF15 mRNA and protein expression by shKIF15. Downregulation of KIF15 inhibited the proliferation and migration of CRC cells while promoting apoptosis. In addition, evidence from the xenograft experiments in nude mice demonstrated that KIF15 knockdown also suppressed tumor growth. Through bioinformatics analysis, the downstream molecular NRAS and Rac signaling pathway associated with KIF15 were identified. KIF15 knockdown was found to inhibit NRAS expression and disrupt Rac signaling pathway. Moreover, WB and Co-IP assays revealed that KIF15 reduced the ubiquitination modification of NRAS protein by interacting with the E3 ligase MDM2, thereby enhancing NRAS protein stability. Functionally, NRAS knockdown was shown to inhibit cell proliferation and migration. In conclusion, KIF15 promoted CRC progression by regulating NRAS expression and Rac signaling pathway.

Keywords: Colorectal cancer, KIF15, NRAS, Rac signaling pathway

Introduction

Colorectal cancer (CRC), which poses clinical challenges, is the third most common cancer worldwide and the most frequent gastrointestinal malignancy, resulting in over 1.2 million newly diagnosed cases annually [1, 2]. Furthermore, CRC ranks as the 4th leading cause of cancer-related deaths, with approximately 694,000 deaths each year [3, 4]. CRC, as a heterogeneous tumor, usually develops by the accumulation of significant genetic changes through the ages, with varying genetic and epigenetic changes [5, 6]. Up to now, in-depth researches have revealed genetic alterations involved in CRC carcinogenesis, including copy number variations, recurrent genetic mutations, chromosomal changes, and epigenetic alterations, many of which occur through the chromosomal instability pathway, which is initiated *via* adenomatous polyposis coli (APC) loss of function [7, 8]. Georg Zeller *et al.* stated that if CRC is diagnosed early and still localized (American Joint Committee on Cancer (AJCC) stages 0, I, or II), the 5-year survival rate is > 80% [9]. However, 50% of all patients with CRC develop metastatic disease, which is associated with a poor prognosis with a 5-year survival rate as low as 13% [10]. At present, the standard treatment regime for advanced CRC is chemotherapy while most current chemotherapeutic drugs cannot distinguish between malignant cells and normal cells, resulting in serious adverse reactions and systemic toxicity, and

the majority of chemotherapeutic drugs are largely ineffective, yet they have been the mainstream of treatment for nearly a decade [11, 12]. Therefore, there is an urgent need to understand the mechanisms that promote cancer development, investigate now therapeutic targets and predict novel biomarkers for treatment outcomes.

Kinesin superfamily proteins (KIFs) are a class of motor proteins which are ubiquitous in eukaryotes [13]. There are 45 KIFs with different functions that have been found in humans, which are divided into 14 categories according to the structural differences [14]. All the KIFs have a highly conserved region of motion providing motion combining with microtubules, thus they can be participate in the movement of a variety of cargoes along microtubules, including organelles, vesicles, protein complexes, mRNAs and chromosomes [15]. Several studies have shown that expression dysregulation of KIFs in the cell cycle may lead to uncontrolled cell growth [14].

KIF15 (also known as Kinesin-12, KSNL7 or HKLP2), a member of KIFs, is a microtubule-based plus-end-directed motor protein that was originally studied for its role in mitosis [16]. It is generally believed that KIF15 regulates the bipolar microtubule spindle apparatus during cells division by generating forces regulating the sliding of microtubules, and these functions of KIF15 exhibit partial functional redundancy with Kinesin-5 (Eg5) [17, 18]. Several studies have confirmed that KIF15 is upregulated in multiple solid malignancies, and is also implicated in various immune diseases *via* inhibiting the endocytic trafficking of α2 integrin [19]. In the study by Wang *et al.*, KIF15 was also shown to promote pancreatic cancer proliferation and identified a potential link between its cancer-promoting effects and the MEK-ERK signaling pathway [20].

Previous studies have primarily focused on examining the function of KIF15 in relation to microtubules, mitosis and other types of cancer. However, the purpose of this study was to explore the crucial role of KIF15 in CRC. We not only demonstrated the interaction between KIF15 and NRAS, which were highly expressed genes in CRC, but also investigated the regulatory mechanism of KIF15 in the progression of CRC.

Material and methods

Clinical samples and cell culture

The colorectal carcinoma (CRC) tissues and the matching para-cancerous tissues were collected at Fudan University Affiliated Tumor Hospital. All CRC patients signed the informed consent forms. Moreover, all experiments involved in this study have been approved by the Ethics committee of the School of Medicine, Fudan University Affiliated Tumor Hospital (050432-4-1212B). All the tissues samples were frozen in liquid nitrogen at -80°C.

Human colorectal carcinoma cell lines RKO and HCT 116 were obtained from American Type Culture Collection (ATCC) and cultured in RPMI 1640 (corning, Corning, NT, USA) with 10% fetal calf serum (FBS) (Invitrogen, Carlsbad, California, USA) at 37°C with 5% CO_2.

Immumohistochemical staining

The samples were sectioned into 5 μm thick paraffin slices. The antigen repair was performed on deparaffinized tissue slices with citrate. The endogenous peroxidase in tissue slices was sealed with 3% H_2O_2 for 5 min, and washed with 1 × PBST three times for 5 min each time. Then slices were sealed with 5% serum for 15 min. The tissue slices were first incubated with the primary antibody at 4°C overnight. After washing with 1 × PBST for three times, tissue slices were incubated with the secondary antibody at 37°C for 1 h. Finally, DAB solution was used for dark staining for 5 min, and hematoxylin was used for redyeing for 15 s. After washing with water, slices were dehydrated using graded alcohol solutions and transparent. The slices were sealed with neutral gum. Finally, the tissue slices were observed under a microscope, and protein expression was evaluated by determining the percentage of positive cells and staining intensity. The positive cell score ranged from 0 to 4, where 0 (negative) indicated no positive signal and < 1% positive cells, while 4 indicated > 75% positive cells. Staining intensity score also ranged from 0 to 3, where 0 (negative) indicated no signal color in cytoplasm, membrane or nucleus and stroma, and 3 indicated dark brown staining. The immumohistochemical staining results were determined by multiplying the positive cell score by staining intensity score. The

higher the score, the higher the antibody expression. The details of primary and secondary antibodies used in this study were provided in Supplementary Table 3.

Lentivirus infection

Using KIF15 or NRAS as templates, interference sequences targeting KIF15 or NRAS were designed, and then inserted into the pHelper lentivirus vector (Shanghai Biostienceres, Co., Ltd., Shanghai, China). Human CRC cells were trypsinized and made into a cell suspension. Then, 1×10^5 cells were seeded into a 6-well plate and cultured with 2 mL lentivirus solution containing shKIF15 or shNRAS (or negative control shRNA). The lentivirus titers were 1×10^6 TU/mL, 2×10^8 TU/mL and 4×10^8 TU/mL, respectively. After 72 h, the fluorescence of green fluorescent protein (GFP) carried by lentivirus was observed under a fluorescence microscope (Olympus, Tokyo, Japan). The interference sequences targeting KIF15 or NRAS were provided in Supplementary Table 1.

qPCR

When the cell density reached 80%, RKO and HCT 116 cells were collected and lysed, and total RNA was extracted by Trizol reagent (Sigma, Missouri, USA). Hiscript QRT supermix for qPCR (+ gDNA WIPER) (Vazyme, Nanjing, China) was used for reverse transcription to obtain cDNA under the guidance of the manufacturer. Real-time PCR was used to detect the mRNA levels of KIF15 and NRAS with GAPDH as internal reference, and the results were calculated with $2^{-\Delta\Delta Ct}$. The real-time PCR reaction system (10 μL) consisted of SYBR Green mastermixs (Q111-02, Vazyme), forward and reverse primers, Dye2, cDNA and RNase-free H_2O. The detection conditions were set as follows: 95°C for 60 s, 45 cycles of 95°C for 10 s and 60°C for 30 s. Then melting-curve analysis was conducted. Primers used in this study were provided in Supplementary Table 2. Each sample was analyzed in triplicate.

Western blotting (WB)

Human CRC cells were lysed by Lysis Buffer, and the protein concentration of cell lysate was measured with BCA Protein Assay Kit (HyClonr-Pierce, Logan, UT, USA). 20 μg proteins were separated by 10% sodium dodecyl sulfate polyacrylamide gel electrophoresis (SDS-PAGE), and then transferred on polyvinylidence fluoride (PVDF) membranes. After blocking with TBST solution containing 5% skim milk overnight at 4°C, PVDF membranes were incubated with primary antibodies for 2 h at room temperature, and washed 3 time with TBST for 10 min each. PVDF membranes were maintained in secondary antibody for 1 h at room temperature. PVDF membranes were colored through Immobilon Western Chemiluminescent HRP Substrote Kit (Millipore, Schwalbach, Germany), and chemiluminescence was performed with Chemiluminescence imaging system (AI600, GE, USA). Finally, PVDF membranes were captured, and the protein bands were analyzed using Image J software to determine the relative expression levels. The details of primary and secondary antibodies used in this study were provided in Supplementary Table 3.

MTT assay

CRC cells were seeded into 96-well plates (2000 cell/well). At day 1, 2, 3, 4 and 5, one of the 96-well plates was treated to detect cell proliferation. Each well was treated with 20 μL 5 mg/mL MTT solution (Genview, Florida, USA) and incubated for 4 h. After removing the culture medium, 100 μL DMSO (Shanghai Shiyi Chemical Reagent Co., Ltd.) was added into each well. The optical density (OD) was measured through a microplate reader (M2009PR, Tecan infinite, Switzerland) at a wavelength of 490 nm. This experiment was repeated three times.

Cell colony assay

CRC cells in the logarithmic phase were trypsinized, resuspended, and counted. Then, 500 cells were seeded into a 6-well plate and cultured for 8 days with medium change every 3 days. 1 mL 4% paraformaldehyde were used to fix CRC cells for 45 min, followed by staining with 500 μL GIEMSA for 15 min. After washing with ddH_2O, images were captured using a digital camera and the colonies were counted. The experiment was performed in triplicate.

Flow cytometer analysis (FCM)

Cell apoptosis was detected by Annexin V-APC apoptosis detection kit (eBioscience, San Diege, CA, USA) according to the manufactur-

er's instructions. RKO and HCT 116 cells were cultured in a 6-well plate. When the cell confluence reached 85%, cells were resuspended and washed with D-Hanks. Cell suspensions were prepared wusing 200 μL 1 × bingding buffer. Cells were stained with 10 μL Annexin V-APC for 10 min at room temperature in the dark. Cell apoptosis was detected using a flow cytometer (Millipore, Schwalbach, Germany). This experiment was conducted in triplicate.

Wound healing

5 × 10^4 RKO or HCT 116 cells were seeded into a 96-well plate. 96 Wounding Replicator (VP408FH, VP scientific) was used for artificial wound in each well, and cells were cultured in RPMI 1640 containing 0.5% FBS. The wound healing of RKO cells was observed at 0 h, 24 h, and 40 h, or 0 h, 24 h, and 48 h, and the wound healing of HCT 116 cells was observed at 0 h, 24 h and 32 h with Cellomics (ArrayScan VT1, Thermo, MA, USA). This experiment was done in triplicate.

Transwell assay

RKO and HCT 116 cells were infected shRNA targeting KIF15 or NRAS or a negative control. Subsequently, the cells were diluted in serum-free medium and counted. A total of 1 × 10^5 cell/well in 100 μL cell suspension were seeded into the upper chamber, while the bottom chamber was filled with 500 μL RPMI 1640 medium containing 30% FBS. After incubating for 24 h, the upper chambers were removed to discard the medium, and any non-metastatic cells were gently wiped off using a cotton swab. The cells on the lower surface of the membrane were then stained for 20 min, washed with water, and air-dried. Finally, the membrane was observed and photographed under a microscope. This experiment was performed in triplicate.

Nude mouse xenograft tumor model

Twenty 4-week-old female BALB/c nude mice were obtained from Shanghai Lingchang Biotechnology Co., Ltd. and randomly divided into 2 groups, 10 mice in each group. After infecting RKO cells in the logarithmic growth stage with shKIF15 or shCrl lentivirus, the cells were resuspended and counted. A total of 4 × 10^6 cells in 200 μL cell suspension were subcutaneously injected into the right arm of each mice. The volume and weight of tumors were measured daily. On the 18th day after the injection of RKO cells, the mice were intraperitoneally injected with 0.7% pentobarbital sodium (SIGMA) at a dose of 10 μL/g. When the mice reached a coma state, in vivo imaging using a live animal imaging system (IVIS Spectrum, Perkin Elmer) was performed to observe the fluorescence intensity. Subsequently, the mice were euthanized with an overdose of 2% pentobarbital sodium. The tumors were surgically removed from the mice and their volume and weight were measured. The tumor volume was calculated using the formula: Tumor volume = π/6 × L × W × W (3.14/6 × L × W × W), where L and W represented the long diameter and short diameter of tumor, respectively. Finally, the tumors were frozen in liquid nitrogen and stored at -80°C. All animal-related experiments described above were approved by the Animal Ethics Committee of the second affiliated hospital of Zhejiang University School of Medicine (No. 161 of 2022).

Primeview human gene expression array and ingenuity pathway analysis (IPA)

Total RNA was extracted from RKO cells infected with negative control or KIF15 shRNA lentivirus, respectively. The quality of the total RNA was evaluated using the Agilent Bioanalyzer 2100 (Agilent, Santa Clara, CA, USA). Based on human GeneChip primeview (Affymetrix, Santa Clara, CA, USA) specification, the total RNA was processed using microarray technology to determine the gene expression in RKO cells. The Limma package in R studio was used for Hierachical clustering difference analysis based on the original microarray data. The *P*-value was calculated using the Right-Tailed Fisher's Exact Test algorithm, and the Benjamin-Hochberg method was used to correct the significant difference level (FDR). Using |Fold Change| ≥ 2.0 and FDR ≤ 0.05 as the screening criteria, the differentially expressed genes in the shKIF15 group were selected.

Ingenuity Pathway Analysis (IPA) was performed on all significantly differentially expressed genes to analyze the significant enrichment of differentially expressed genes in classical pathways and diseases and functions, as well as to build the interaction network between signaling pathways and molecules.

Protein stability assay

Cycloheximide (CHX, 0.2 mg/mL, S7418, Selleck), an inhibitor of protein synthesis, was used to treat RKO cells with KIF15 knockdown or MDM2 overexpression in order to inhibit protein translation. RKO cells were lysed at 0, 2, 4, and 8 h to extract total protein. Then 20 μg total protein was taken out and subjected to WB to detect the levels of NRAS protein. Information on relevant primary and secondary antibodies was provided in Supplementary Table 3.

In vivo ubiquitination assay

After shKIF15 or MDM2 overexpression lentivirus infected RKO cells for 24 h, MG-132 (20 μM, HY-13259, MEC), an inhibitor of the ubiquitin-proteasome pathway, was added into the culture medium for 6 h. RKO cells were collected and lysed to obtain total protein. 20 μg total protein was subjected to WB to detect the levels of NRAS protein. Additionally, 1.0 mg total protein and an appropriate amount of antibody were incubated at 4°C overnight, and then incubated with 20 μL beads at 4°C for 2 h. The protein-antibody-beads complex was washed twice with IP lysis buffer, and then subjected to WB to determine the levels of ubiquitin with ubiquitin antibody. Information on relevant primary and secondary antibodies was provided in Supplementary Table 3.

Co-immunoprecipitation (Co-IP)

RKO cells infected with KIF15 overexpression lentivirus were harvested and lysed on ice using pre-chilled IP lysis buffer for 5 min. BCA Protein Assay Kit was applied to measure the protein concentration. 1.0 mg protein was incubated with the appropriate amount of antibody at 4°C overnight, and then incubated with 20 μL beads at 4°C for 2 h. The protein-antibody-beads complex was washed twice with IP lysis buffer and subjected to SDS-PAGE. The separated protein was transferred to PVDF membranes. The membranes were sealed with TBST containing 5% skimmed milk at room temperature for 1 h. Primary antibodies were incubated with the membranes at 4°C overnight, and secondary antibodies were incubated with membranes at room temperature for 2 h. After washing 3 times with 1 × TBST, the chemiluminescence method was used for color development, and a chemiluminescence imaging system (GE) was used for imaging protein bands. Information on the relevant primary and secondary antibodies was provided in Supplementary Table 3.

Celigo cell counting assay

RKO and HCT 116 cells in the logarithmic growth stage were trypsinized and resuspended. Cells were seeded into 96-well plates with 2000 cells per well. The Celigo (Nexcelom, Massachusetts, USA) was used to scan the same field of the 96-well plate at the same time for 5 consecutive days to obtain scanning images. The cells in the scanning images were counted using Image J, and then statistical analysis was performed. The experiment was repeated three times.

Statistical analysis

All data in this study were analyzed using SPSS 17.0 (OBM), and graphs were created using GraphPad prism 6 software (San Diego, CA, USA). The data obtained from cell and animal experiments were presented as the mean ± standard deviation (SD). The sign test was used to statistically analyze the expression level of KIF15 in colorectal carcinoma and para-carcinoma tissues. Mann-Whitney U analysis was conducted to analyze the difference between KIF15 gene expression and tumor characteristics. Pearson correlation analysis was performed to evaluate the correlation between KIF15 expression and pathological grade. T-test was used to determine statistical differences and $P < 0.05$ was accepted as statistically significant.

Results

The levels of KIF15 are upregulated in colorectal carcinoma (CRC) tissues and are connected to the stage of CRC

Immumohistochemical staining were performed on tumor tissues and para-carcinoma tissues from CRC patients. Representative pictures demonstrating significant upregulation of KIF15 in CRC tissues were shown in **Figure 1A**. Similar results were obtained when comparing the expression of KIF15 in CRC tissues and para-carcinoma tissues with immunohistochemistry (**Table 1**). Both the statistical analy-

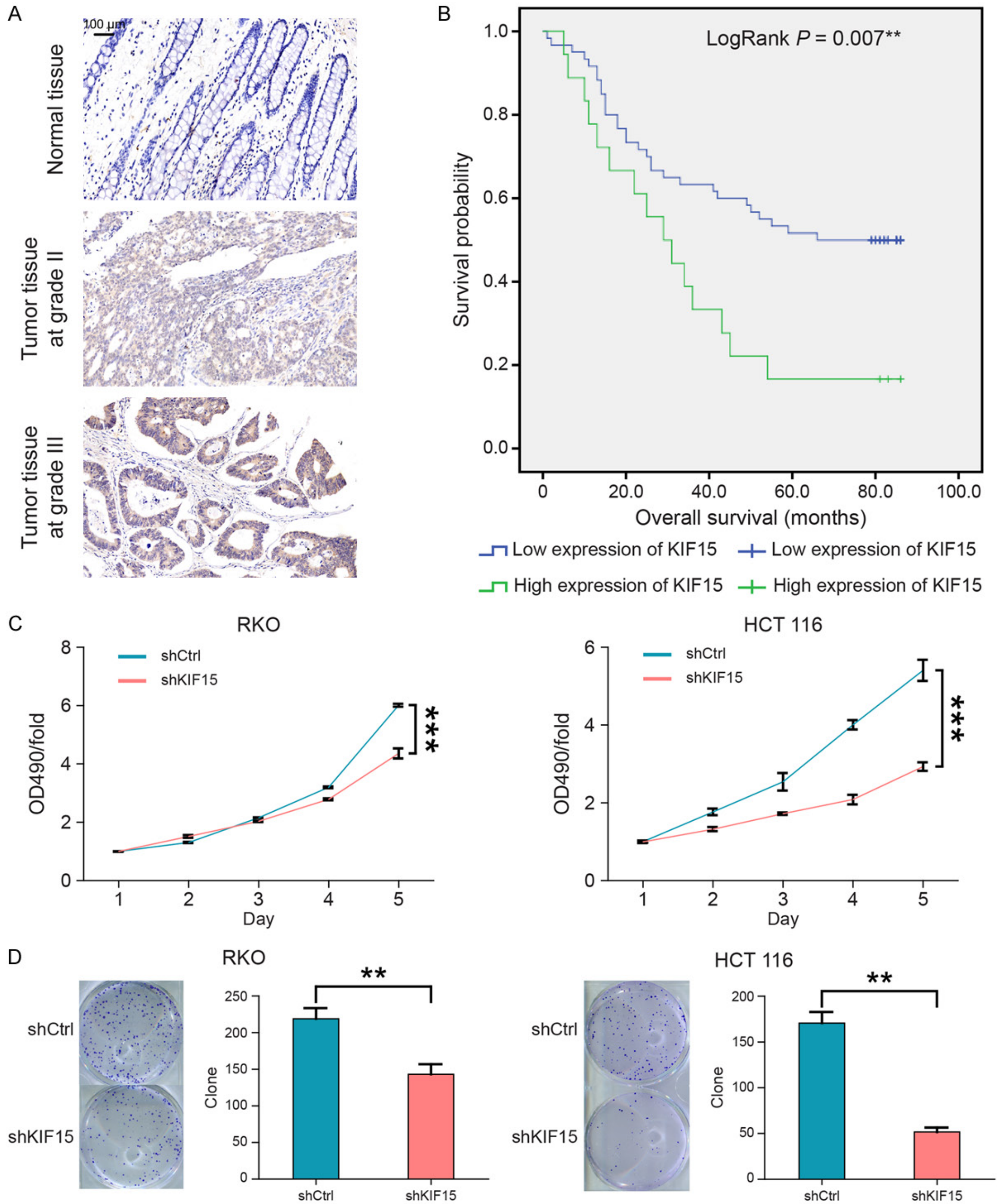

Figure 1. The levels of KIF15 in CRC tissues and the effects of KIF15 on CRC cell proliferation. A. The levels of KIF15 in CRC tissues with different stages and adjacent normal tissues were analyzed by immumohistochemical staining. Magnification times: 200 ×. B. Kaplan-Meier survival analysis revealed a relationship between KIF15 levels and overall survival of CRC patients. Data and information of survival analysis were obtained from tissue chip, including 60 cases with high expression of KIF15 and 18 cases with low expression of KIF15. C. The fold changes of absorbance of KIF15 knockdown CRC cells at 490 nm with time were measured by MTT assay, so as to assess the effects of KIF15 on cell proliferation. T test was used to performed statistical analysis on the last detection results. D. Colony formation assay was used for analyzing the colony formation ability of CRC cells infected with shRNA-lentivirus. Statistical analysis of the detection results between the two groups was conducted using t test. ShCtrl: CRC cells infected with negative control shRNA lentivirus; shKIF15: CRC cells infected with KIF15-shRNA lentivirus. $^{**}P < 0.01$, $^{***}P < 0.001$.

Table 1. Expression patterns in colorectal cancer tissues and para-carcinoma tissues revealed in immunohistochemistry analysis

KIF15 expression	Tumor tissue		Para-carcinoma tissue		*P* value
	Cases	Percentage	Cases	Percentage	
Low	18	23.1%	74	100%	< 0.001***
High	60	76.9%	0	-	

Note: ***P < 0.001.

Table 2. Relationship between KIF15 expression and tumor characteristics in patients with colorectal cancer

Features	No. of patients	KIF15 expression		*P* value
		Low	High	
All patients	78	18	60	
Age (years)				0.470
< 69	37	10	27	
≥ 69	40	8	32	
Gender				0.487
Male	44	9	35	
Female	33	9	24	
Grade				0.035*
II	59	17	42	
III	19	1	18	
T Infiltrate				0.760
T2	3	0	3	
T3	53	14	39	
T4	22	4	18	
Lymphatic metastasis (N)				0.324
N0	38	11	27	
N1	32	5	27	
N2	8	2	6	
AJCC stage				0.218
1	3	0	3	
2	34	11	23	
3	37	7	30	
4	4	0	4	
Tumor size				0.509
< 5 cm	25	7	18	
≥ 5 cm	52	11	41	

Note: *P < 0.05.

sis and Pearson correlation analysis of KIF15 expression and tumor characteristics in CRC patients suggested a positive correlation between KIF15 expression and the pathological grade (**Tables 2**, **3**). Additionally, Kaplan-Meier analysis showed that high expression of KIF15 was associated with lower overall survival, indicating the potential of KIF15 as a prognostic marker for CRC (**Figure 1B**).

KIF15 knockdown suppresses CRC both in vitro and in vivo

For the reason of further investigating the role of KIF15 in CRC cells, KIF15 knockdown cell models were created by infecting lentivirus carrying KIF15-shRNA. The infection efficiency was demonstrated to be over 80% by observing the fluorescence expression of green fluorescent protein (GFP) carried by lentivirus vectors (Supplementary Figure 1A). Simultaneously, the mRNA and protein levels of KIF15 were significantly downregulated after KIF15-shRNA infection, as detected by qPCR and WB, respectively (Supplementary Figure 1B, 1C). Hence, CRC cells with KIF15 knockdown were successfully generated.

Based on further analysis, the proliferation speeds of CRC cells were obviously slowed down following KIF15 downregulation (**Figure 1C**). The colony formation assay yielded similar results, indicating that downregulation of KIF15 inhibited CRC cell proliferation (**Figure 1D**). As shown in **Figure 2A**, the cell apoptosis rates were distinctly increased after downregulating KIF15. Furthermore, based on the detection results of the Human Apoptosis Antibody Array, the protein levels of Bax, CD40L, cytoC, IGFBP-1 and IGFBP-4 were significantly increased in the shKIF15 group, while IGF-1, Survivin, TRAILR-3 and XIAP were significantly decreased. These findings suggested that the depletion of KIF15 might induce apoptosis by regulating these proteins (**Figure 2B** and Supplementary Figure 2A, 2B).

Table 3. The correlation between KIF15 expression and pathological grade in patients with colorectal cancer

		KIF15
Grade	Pearson correlation	0.240
	Significance (double tails)	0.034*
	N	78

Note: *P < 0.05.

Both wound healing and transwell assays revealed that knockdown of KIF15 suppressed the migration of CRC cells (**Figure 2C**, **2D**). To sum up, we preliminarily demonstrated that KIF15 knockdown inhibited the proliferation and migration of CRC cells while promoting apoptosis.

Furthermore, the effects of KIF15 on CRC were also investigated *in vivo*. According to the representative image obtained from in vivo imaging in nude mice and the total fluorescence intensity, it was observed that tumors were suppressed following KIF15 knockdown (**Figure 3A**, **3B**). Besides, the volume and weight of tumors in the shKIF15 group were smaller than those in the shCtrl group (**Figure 3C-E**). These results indicated that KIF15 knockdown effectively suppressed tumor growth *in vivo*.

KIF15 regulates the stability of NRAS protein and activates the Rac signaling pathway in CRC

Gene expression profiling was performed on RKO cells infected with shCtrl or shKIF15 using Genechip, and significantly differentially expressed genes were identified using threshold criteria of |Fold Change| ≥ 2.0 and P < 0.05. In the shKIF15 group, 833 genes were obviously upregulated and 1416 genes were downregulated (Supplementary Figure 3A). Notably, NRAS was found to be significantly downregulated by shKIF15. Subsequent IPA analysis revealed enrichment of differentially expressed genes in classical signaling pathways (Supplementary Figure 3B). Specifically, Rac signaling pathway was inhibited in KIF15 knockdown CRC cells, with most of the genes in this pathway being downregulated in the shKIF15 group (Supplementary Figure 3C). The interaction network further revealed that downregulated NRAS interacted with some proteins in the Rac signaling pathway, suggesting a potential relationship among KIF15, NRAS and Rac signaling pathway (**Figure 4A**). Therefore, NRAS and Rac signaling pathway were considered the downstream gene and pathway of KIF15, further investigations into their roles in CRC progression were warranted. Immumohistochemical staining results demonstrated that NRAS was upregulated in CRC tissues as expected (**Figure 4B**). Additionally, silencing KIF15 led to the inhibition of related proteins in the Rac signaling pathway, such as ELK1, p-ELK1, p-ERK1/2 and Ras, consistent with the predictions of bioinformatics analysis (**Figure 4C**). However, the specific mechanism by which KIF15 regulated the expression of NRAS remained unclear, and required further research.

Ubiquitination is a versatile protein modification system that is involved in almost all aspects of eukaryotic biology [21]. Ubiquitin-modified proteins play an important role in determining cell fate and function, and abnormal ubiquitination is often associated with birth defects, pediatric diseases and cancer [22]. In this study, we observed that NRAS protein levels decreased more rapidly in the KIF15 knockdown group compared with the control group after treatment with CHX, indicating that KIF15 downregulation destabilized NRAS protein (**Figure 4D**). Treatment with the proteasome inhibitor MG-132 partially alleviated the downregulation of NRAS protein caused by KIF15 knockdown in RKO cells (**Figure 4E**). Besides, KIF15 knockdown markedly increased the levels of ubiquitination modification of NRAS (**Figure 4F**). These findings suggested that KIF15 enhanced the stability of NRAS protein through the proteasome-ubiquitin pathway. Nevertheless, no direct interaction was observed between KIF15 and NRAS.

Previous reports have suggested that ubiquitination modification is typically achieved through the involvement of E1, E2 and E3 enzymes. The E3 ligase connects ubiquitin to the target protein, leading to its degradation by the proteasome [23]. Based on this, we hypothesized that KIF15 might interact with ubiquitin ligase to modulate the ubiquitination modification of NRAS protein. To explore this, we utilized the UbiBrowser database to predict the E3 ligase responsible for interacting with NRAS, and found a strong association between NRAS and MDM2 (**Figure 4G**). Furthermore, Co-IP assay results demonstrated the interaction

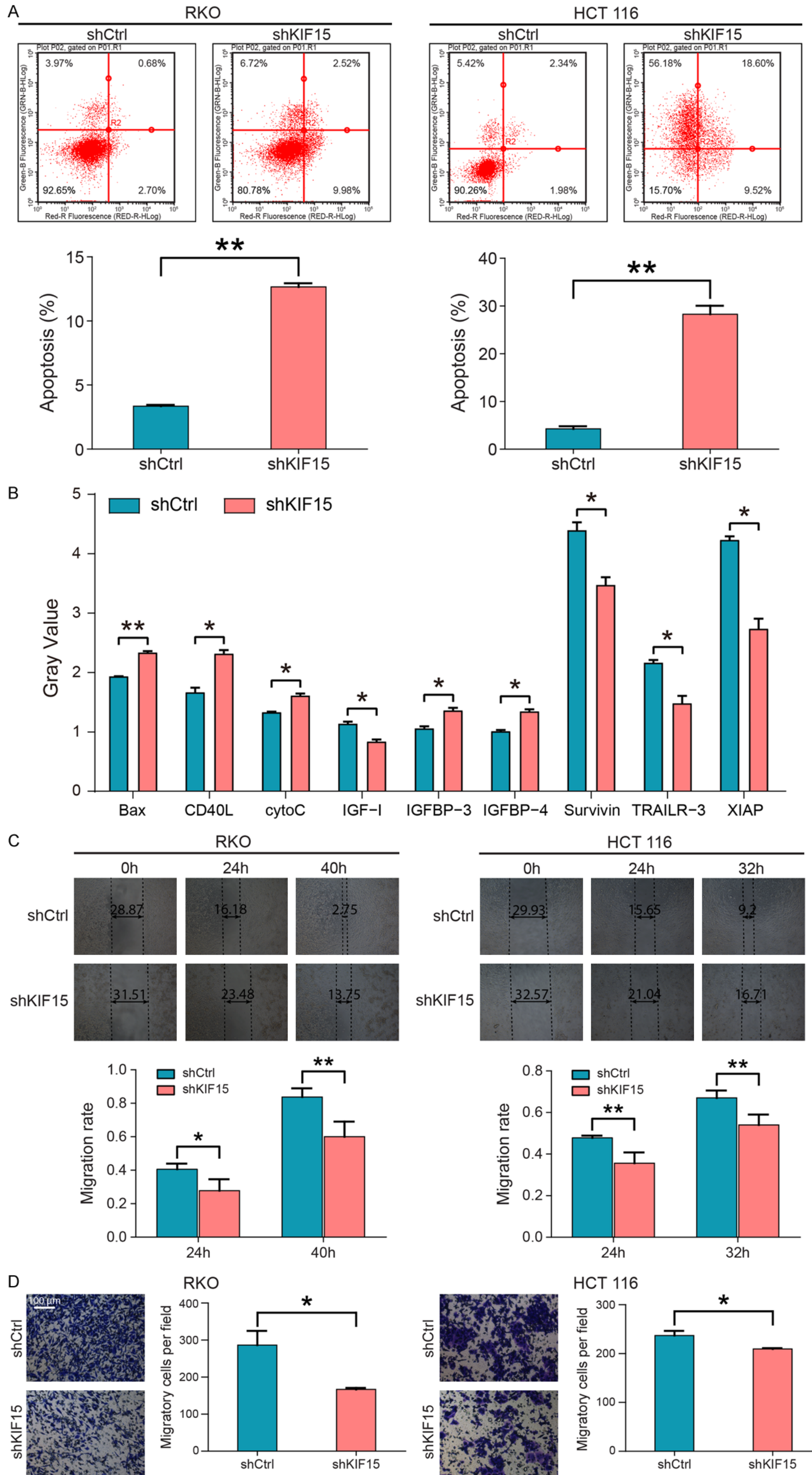
A
RKO
HCT 116
shCtrl
shKIF15
3.97%
0.68%
92.65%
2.70%
6.72%
2.52%
80.78%
9.98%
5.42%
2.34%
90.26%
1.98%
56.18%
18.60%
15.70%
9.52%
Apoptosis (%)
**
B
shCtrl
shKIF15
Gray Value
Bax
CD40L
cytoC
IGF-I
IGFBP-3
IGFBP-4
Survivin
TRAILR-3
XIAP
C
RKO
HCT 116
0h
24h
40h
32h
28.87
16.18
2.75
31.51
23.48
13.75
29.93
15.65
9.2
32.57
21.04
16.71
Migration rate
D
RKO
HCT 116
Migratory cells per field
100 μm

Figure 2. KIF15 knockdown promoted CRC cells apoptosis and suppressed migration. A. CRC cells apoptosis was verified to be promoted after KIF15 knockdown by FACS. The upper and lower left regions were normal infected with lentivirus; the upper and lower right regions were apoptosis cells infected with lentivirus. Statistical analysis of the detection results between the two groups was conducted using t test. B. According to the detection results of Human Apoptosis Antibody Array, the gray value of proteins with significant changes were shown in the histogram. Statistical analysis of the detection results between the two groups was conducted using t test. C. Results of wound healing assay indicated a negative effect of KIF15 knockdown on CRC cells migration. Statistical analysis of the detection results between the two groups was conducted using t test. D. The influence of downregulated KIF15 on CRC cells metastasis was also confirmed by transwell assay. Statistical analysis of the detection results between the two groups was conducted using t test. ShCtrl: CRC cells infected with negative control shRNA lentivirus; shKIF15: CRC cells infected with KIF15-shRNA lentivirus. $*P < 0.05$, $**P < 0.01$.

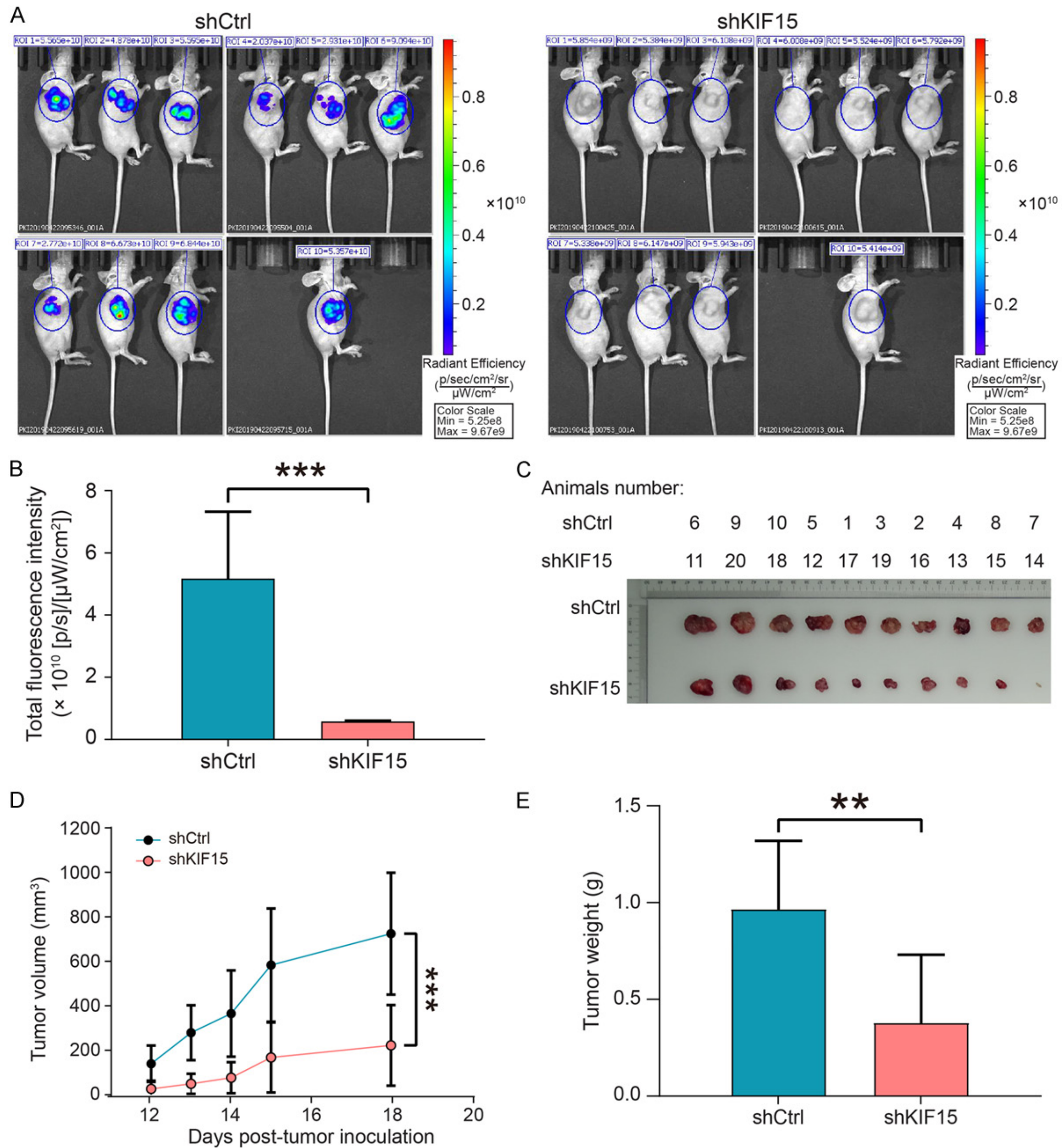

Figure 3. The effects of KIF15 knockdown on CRC were verified *in vivo*. A. Representative images of in vivo imaging in nude mice. B. Total fluorescence intensify was determined by in vivo imaging to analyze tumor growth *in vivo*. Statistical analysis of the detection results between the two groups was conducted using t test. C. The solid tumors in nude mice were removed from nude mice after sacrifice, and then photographed. D. The volume of tumors was measured by Vernier caliper, and the results indicated that KIF15 knockdown suppressed tumor growth. T test was

used for statistical analysis on the last detection results. E. Compared with the control group, the tumor weight was lighter in the KIF15 downregulated group. Statistical analysis of the detection results between the two groups was conducted using t test. ShCtrl: CRC cells infected with negative control shRNA lentivirus; shKIF15: CRC cells infected with KIF15-shRNA lentivirus. $^{**}P < 0.01$, $^{***}P < 0.001$.

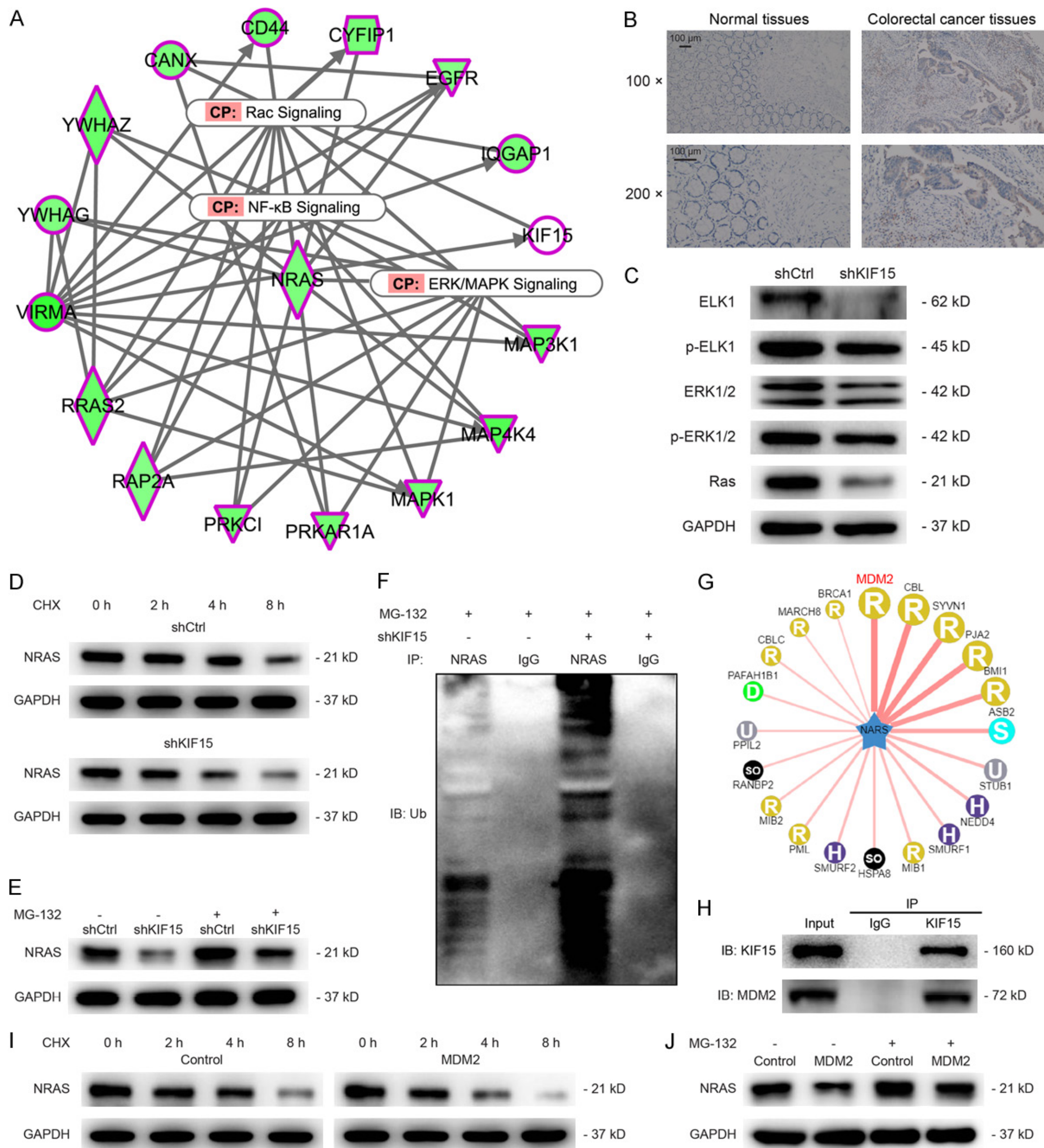

Figure 4. IPA was used to analyze the gene interacting with KIF15 and the signaling pathway regulated by KIF15. A. The interaction network showed the relationship among KIF15, NRAS and Ras signaling pathway. B. The expression of NRAS was verified to be upregulated in CRC tissues by immumohistochemical staining. Magnification times: 100 × and 200 ×. C. WB was performed to detect levels of proteins involved in Ras signaling pathway. D. CHX was applied to treat the KIF15 knockdown RKO cells, and WB was performed to detect the levels of NRAS protein at 0, 2, 4, and 8 h. CHX: 0.2 mg/mL. E. MG-132 treated KIF15 knockdown RKO cells for 6 h, and then the levels of NRAS protein were detected by WB. MG-132: 20 μM. F. After treating RKO cells infected with shKIF15 or shCtrl lentivirus with MG-132, IP assay was performed to detect the ubiquitination level of NRAS protein. G. UbiBrowser database was used to predict human ubiquitin ligase (E3) targeting NRAS protein. H. Co-IP assay was used to confirm the interaction between KIF15 and MDM2. I. CHX was applied to treat the MDM2 overexpression RKO cells, and WB was performed to detect the levels of NRAS protein at 0, 2, 4, and 8 h. J. MG-132 treated MDM2 overexpression

RKO cells for 6 h, and then the levels of NRAS protein were detected by WB. ShCtrl: CRC cells infected with negative control shRNA lentivirus; shKIF15: CRC cells infected with KIF15-shRNA lentivirus. MDM2: MDM2 overexpression RKO cells.

between MDM2 and KIF15 (**Figure 4H**). To confirm these findings, RKO cells in both the control group and MDM2 group were treated with CHX, and NRAS protein was detected using WB. The results indicated that overexpression of MDM2 reduced the stability of NRAS protein (**Figure 4I**). Moreover, MDM2 overexpression inhibited the expression of NRAS protein, but this effect was alleviated by treatment with MG-132 (**Figure 4J**). Consequently, the downregulation of KIF15 disrupted the stability of NRAS protein by interacting with MDM2, subsequently impacting the protein levels within CRC cells.

KIF15 promotes CRC cells proliferation and migration and inhibits cell apoptosis by interacting with NRAS

For the purpose of investigating the role of NRAS in CRC, three interference sequences targeting NRAS were employed to generate NRAS knockdown CRC cells. qPCR results indicated that shNRAS-3 exhibited the best knockdown efficiency and therefore, it was chosen for subsequent study (Supplementary Figure 4A). The infection efficiency was confirmed to be over 80% by observing the expression of GFP (Supplementary Figure 4B). Both mRNA and protein levels of NRAS were significantly downregulated following infection with NRAS-shRNA or NRAS-shRNA along with KIF15-shRNA lentiviruses (Supplementary Figure 4C, 4D). Additionally, KIF15 was also downregulated in the shNRAS+shKIF15 group. Hence, successful knockdown of NRAS or both NRAS and KIF15 in CRC cells were achieved.

Celigo cell counting assay results showed that silencing NRAS suppressed CRC cell proliferation. Interestingly, a more pronounced suppression effect was observed when both NRAS and KIF15 were simultaneously silenced (Supplementary Figure 5 and **Figure 5A**), consistent with the results of the colony formation assay. Whether NRAS or KIF15 was silenced, the colony formation ability of CRC cells was inhibited (**Figure 5B**). Moreover, downregulation of NRAS resulted in an increased apoptosis rate of CRC cells (**Figure 5C**). Additionally, both wound healing and transwell assays manifested that silencing NRAS restrained the migration of CRC cells, with a stronger inhibitory effect observed in CRC cells co-infected with shNRAS and shKIF15 lentiviruses (**Figure 5D**, **5E**).

Discussion

CRC is the third most common malignant cancer and the second leading cause of cancer-related death globally [24]. Specifically, in China, it is estimated that more than 3.8 million new cancer cases of CRC are detected annually [25]. Despite recent advancements in therapy, CRC remains incurable due to the molecular heterogeneity of tumor cells [26]. Therefore, it is crucial to discover new treatment strategies for CRC. In this particular study, it was found that KIF15 was highly expressed in CRC tissues and there was a positive correlation between KIF15 expression and the pathological grade. KIF15 is a member of KIFs and plays a critical role in the assembly and maintenance of the mitotic spindle [18]. It also plays a crucial role in various tumors. Overexpression of KIF15 was negatively correlated with the survival of patients with mesenchymal glioblastoma multiforme subtype [27]. KIF15 was also overexpressed in breast cancer cells and held great values as a prognostic factor and potential therapeutic target for endocrine therapy-resistant breast cancer [20]. This study suggested that high expression of KIF15 was predictive of poor prognosis in CRC patients, prompting further investigation into its role in CRC progression.

Previous studies reported that KIF15 was memorably upregulated in human lung tumor tissues, and downregulation of KIF15 induced cell cycle arrest at the G1/S phase, suppressing cell growth [28]. In this study, successful knockdown of KIF15 was achieved *in vitro* in CRC cells, and further studies demonstrated that downregulation of KIF15 inhibited CRC cell proliferation and migration, while promoting cell apoptosis. Furthermore, KIF15 knockdown suppressed tumor growth in nude mice. The mechanism behind KIF15's role in cancer has studied, with evidence showing its interac-

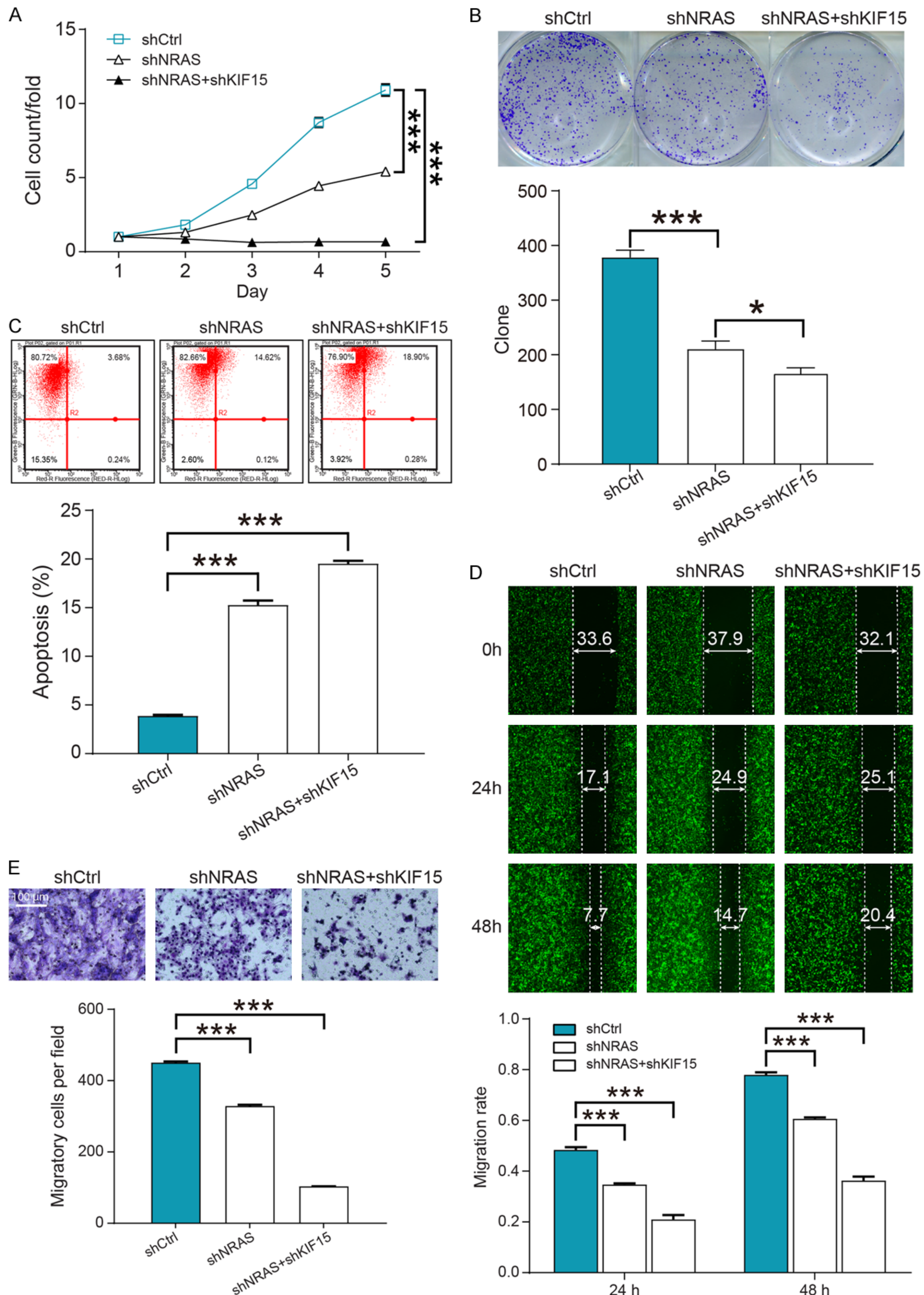

Figure 5. Both KIF15 and NRAS knockdown suppressed CRC cell proliferation and migration but promoted cell apoptosis. A. The fold changes of CRC cell count with time were measured by Celigo cell counting assay, so as to assess the effects of KIF15 or NRAS on cell proliferation. T test was used to performed statistical analysis on the last detection results. B. Colony formation assay was used for analyzing the colony formation ability of CRC cells infected

with shRNA-lentivirus. Statistical analysis of the detection results between the two groups was conducted using t test. C. CRC cells apoptosis was determined by FACS, which revealed a promoting effect of NRAS downregulation. Statistical analysis of the detection results between the two groups was conducted using t test. D. Results of wound healing assay indicated that there was a negative effect of NRAS knockdown on CRC cells migration. Statistical analysis of the detection results between the two groups was conducted using t test. E. The influence of NRAS on CRC cells metastasis was also confirmed by transwell assay. Statistical analysis of the detection results between the two groups was conducted using t test. ShCtrl: CRC cells infected with negative control shRNA lentivirus; shNRAS: CRC cells infected with NRAS-shRNA lentivirus; shNRAS+shKIF15: CRC cells infected with NRAS- and KIF15-shRNA lentivirus. ***$P < 0.001$.

tion with phosphor-glycerate dehydrogenase (PHGDH) and inhibition of PHGDH degradation by proteasome, thereby promoting the phenotype and malignancy of cancer stem cells in hepatocellular carcinoma [29]. However, based on sequencing data from KIF15 knockdown CRC cells, this study conducted bioinformatics analysis and identified NRAS as the downstream gene and Rac signaling pathway as the downstream pathway of KIF15 in CRC.

Neuroblastoma RAS viral oncogene homolog (NRAS) is a member of the human RAS gene family, encoding GTPase that participates in regulating cell division and has been identified as an oncogene [30]. In the study, the downregulation of KIF15 caused a downregulation of NRAS protein, but there was no direct relationship between KIF15 and NRAS proteins. Studies showed that KIF15 reduced the ubiquitination modification of the target protein by enhancing the binding of deubiquitination enzymes to the target protein, thereby enhancing the stability of the target protein [31, 32]. Ubiquitination is a common method of protein post-translational modification that regulates the stability, function, positioning and protein-protein interactions of substrates [33]. Therefore, we hypothesized that KIF15 affected the level of NRAS protein by regulating the ubiquitination of NRAS. After treatment with CHX, KIF15 knockdown significantly weakened the stability of NRAS protein. Downregulation of KIF15 limited the expression of NRAS protein, which was reversed by MG-132. Additionally, KIF15 knockdown also increased the ubiquitination modification of NRAS protein. These findings indicated that KIF15 indeed affected the ubiquitination modification of NRAS protein. Ubiquitination is sequential process involving E1 activation, E2 binding and E3 ligase activity [34]. Analysis of the UbiBrowser database revealed a strong interaction between NRAS and MDM2. MDM2 was an E3 ligase that was overexpressed in many cancers and promoted proteasome-mediated degradation of target proteins through binding [35, 36]. Co-IP assay suggested that MDM2 also interacted with KIF15. Furthermore, overexpression of MDM2 in RKO cells impaired the stability of NRAS protein. In CRC cells, the downregulation of NRAS protein by MDM2 overexpression was restored after MG-132 treatment. Therefore, KIF15 affected the stability of NRAS protein by regulating MDM2-mediated ubiquitination modification, thereby increasing NRAS protein levels in CRC cells.

Studies showed that NRAS, through its GTPase enzymatic site, acted as a molecular switch to transmit extracellular signals to transcription factors and cyclins in the nucleus, thereby triggering cell growth, differentiation, proliferation, and survival [37]. Nevertheless, previous reports mainly focused on the effects of NRAS mutation on CRC. NRAS mutations were demonstrated to lead to an overactive RAS signaling pathway, thus predicting poor prognosis and adverse reactions to anti-EGFR treatment [38]. The results of this study revealed that silencing NRAS suppressed CRC cell proliferation and migration, and increased apoptosis. When both KIF15 and NRAS were downregulated, the inhibitory effects on cell proliferation and migration were more significant. Furthermore, KIF15 knockdown inhibited the expression of ELK1, p-ELK1, p-ERK1/2 and Ras proteins involved in Rac signaling pathway.

This study explored the high expression of KIF15 in CRC and revealed the inhibitory effects of KIF15 knockdown on the progression of CRC. Moreover, we preliminarily demonstrated that KIF15 influenced CRC by regulating NRAS expression. However, there are some limitations in this study. Firstly, we did not investigate whether KIF15 affected the apoptosis of CRC cells by regulating the expression of Bax, CD40L, cytoC, IGFBP-1 and IGFBP-4. Secondly, a larger clinical sample size is needed to testify

the expression and correlation of KIF15 and NRAS. In conclusion, KIF15, an oncogene, was associated with a poor prognosis of CRC and affected the stability of NRAS protein through MDM2-mediated ubiquitination modification, thus promoting the progression of CRC. KIF15 may hold potential as a target for the treatment and prognosis of CRC.

Acknowledgements

This study was supported by the National Natural Science Foundation of China (Grant Nos. 81672364, 81871917).

Disclosure of conflict of interest

None.

Address correspondence to: Shaojun Yu, Department of Colorectal Surgery and Oncology, Key Laboratory of Cancer Prevention and Intervention, Ministry of Education, The Second Affiliated Hospital, Zhejiang University School of Medicine, 88th, Jiefang Road, Hangzhou 310000, Zhejiang, China. Tel: +86-18658160889; E-mail: jackdavid1982@zju.edu.cn

References

[1] Sun G, Li Y, Peng Y, Lu D, Zhang F, Cui X, Zhang Q and Li Z. Identification of a five-gene signature with prognostic value in colorectal cancer. J Cell Physiol 2019; 234: 3829-3836.

[2] Ma Y, Zhan S, Lu H, Wang R, Xu Y, Zhang G, Cao L, Shi T, Zhang X and Chen W. B7-H3 regulates KIF15-activated ERK1/2 pathway and contributes to radioresistance in colorectal cancer. Cell Death Dis 2020; 11: 824.

[3] Hugen N, Brown G, Glynne-Jones R, de Wilt JH and Nagtegaal ID. Advances in the care of patients with mucinous colorectal cancer. Nat Rev Clin Oncol 2016; 13: 361-369.

[4] Urban BC, Collard TJ, Eagle CJ, Southern SL, Greenhough A, Hamdollah-Zadeh M, Ghosh A, Poulsom R, Paraskeva C, Silver A and Williams AC. BCL-3 expression promotes colorectal tumorigenesis through activation of AKT signalling. Gut 2016; 65: 1151-1164.

[5] Sebastian C and Mostoslavsky R. Untangling the fiber yarn: butyrate feeds Warburg to suppress colorectal cancer. Cancer Discov 2014; 4: 1368-1370.

[6] Hamada T, Cao Y, Qian ZR, Masugi Y, Nowak JA, Yang J, Song M, Mima K, Kosumi K, Liu L, Shi Y, da Silva A, Gu M, Li W, Keum N, Zhang X, Wu K, Meyerhardt JA, Giovannucci EL, Giannakis M, Rodig SJ, Freeman GJ, Nevo D, Wang M, Chan AT, Fuchs CS, Nishihara R and Ogino S. Aspirin use and colorectal cancer survival according to tumor CD274 (programmed cell death 1 ligand 1) expression status. J Clin Oncol 2017; 35: 1836-1844.

[7] Fujii M, Shimokawa M, Date S, Takano A, Matano M, Nanki K, Ohta Y, Toshimitsu K, Nakazato Y, Kawasaki K, Uraoka T, Watanabe T, Kanai T and Sato T. A colorectal tumor organoid library demonstrates progressive loss of niche factor requirements during tumorigenesis. Cell Stem Cell 2016; 18: 827-838.

[8] Zajac O, Raingeaud J, Libanje F, Lefebvre C, Sabino D, Martins I, Roy P, Benatar C, Canet-Jourdan C, Azorin P, Polrot M, Gonin P, Benbarche S, Souquere S, Pierron G, Nowak D, Bigot L, Ducreux M, Malka D, Lobry C, Scoazec JY, Eveno C, Pocard M, Perfettini JL, Elias D, Dartigues P, Goere D and Jaulin F. Tumour spheres with inverted polarity drive the formation of peritoneal metastases in patients with hypermethylated colorectal carcinomas. Nat Cell Biol 2018; 20: 296-306.

[9] Zeller G, Tap J, Voigt AY, Sunagawa S, Kultima JR, Costea PI, Amiot A, Bohm J, Brunetti F, Habermann N, Hercog R, Koch M, Luciani A, Mende DR, Schneider MA, Schrotz-King P, Tournigand C, Tran Van Nhieu J, Yamada T, Zimmermann J, Benes V, Kloor M, Ulrich CM, von Knebel Doeberitz M, Sobhani I and Bork P. Potential of fecal microbiota for early-stage detection of colorectal cancer. Mol Syst Biol 2014; 10: 766.

[10] Tabernero J, Yoshino T, Cohn AL, Obermannova R, Bodoky G, Garcia-Carbonero R, Ciuleanu TE, Portnoy DC, Van Cutsem E, Grothey A, Prausova J, Garcia-Alfonso P, Yamazaki K, Clingan PR, Lonardi S, Kim TW, Simms L, Chang SC and Nasroulah F; RAISE Study Investigators. Ramucirumab versus placebo in combination with second-line FOLFIRI in patients with metastatic colorectal carcinoma that progressed during or after first-line therapy with bevacizumab, oxaliplatin, and a fluoropyrimidine (RAISE): a randomised, double-blind, multicentre, phase 3 study. Lancet Oncol 2015; 16: 499-508.

[11] Wu CH, Kuo YH, Hong RL and Wu HC. Alpha-enolase-binding peptide enhances drug delivery efficiency and therapeutic efficacy against colorectal cancer. Sci Transl Med 2015; 7: 290ra91.

[12] Dow LE, O'Rourke KP, Simon J, Tschaharganeh DF, van Es JH, Clevers H and Lowe SW. Apc restoration promotes cellular differentiation and reestablishes crypt homeostasis in colorectal cancer. Cell 2015; 161: 1539-1552.

[13] Camlin NJ, McLaughlin EA and Holt JE. Motoring through: the role of kinesin superfamily proteins in female meiosis. Hum Reprod Update 2017; 23: 409-420.
[14] Lucanus AJ and Yip GW. Kinesin superfamily: roles in breast cancer, patient prognosis and therapeutics. Oncogene 2018; 37: 833-838.
[15] Willemsen MH, Ba W, Wissink-Lindhout WM, de Brouwer AP, Haas SA, Bienek M, Hu H, Vissers LE, van Bokhoven H, Kalscheuer V, Nadif Kasri N and Kleefstra T. Involvement of the kinesin family members KIF4A and KIF5C in intellectual disability and synaptic function. J Med Genet 2014; 51: 487-494.
[16] Feng J, Hu Z, Chen H, Hua J, Wu R, Dong Z, Qiang L, Liu Y, Baas PW and Liu M. Depletion of kinesin-12, a myosin-IIB-interacting protein, promotes migration of cortical astrocytes. J Cell Sci 2016; 129: 2438-2447.
[17] Dong Z, Wu S, Zhu C, Wang X, Li Y, Chen X, Liu D, Qiang L, Baas PW and Liu M. Clustered regularly interspaced short palindromic repeats (CRISPR)/Cas9-mediated kif15 mutations accelerate axonal outgrowth during neuronal development and regeneration in zebrafish. Traffic 2019; 20: 71-81.
[18] Drechsler H and McAinsh AD. Kinesin-12 motors cooperate to suppress microtubule catastrophes and drive the formation of parallel microtubule bundles. Proc Natl Acad Sci U S A 2016; 113: E1635-44.
[19] Menyhart O, Pongor LS and Gyorffy B. Mutations defining patient cohorts with elevated PD-L1 expression in gastric cancer. Front Pharmacol 2019; 9: 1522.
[20] Wang J, Guo X, Xie C and Jiang J. KIF15 promotes pancreatic cancer proliferation via the MEK-ERK signalling pathway. Br J Cancer 2017; 117: 245-255.
[21] Manitta VJ, Philip JA and Cole-Sinclair MF. Palliative care and the hemato-oncological patient: can we live together? A review of the literature. J Palliat Med 2010; 13: 1021-1025.
[22] Rape M. Ubiquitylation at the crossroads of development and disease. Nat Rev Mol Cell Biol 2018; 19: 59-70.
[23] Song L and Luo ZQ. Post-translational regulation of ubiquitin signaling. J Cell Biol 2019; 218: 1776-1786.
[24] Han K, Wang FW, Cao CH, Ling H, Chen JW, Chen RX, Feng ZH, Luo J, Jin XH, Duan JL, Li SM, Ma NF, Yun JP, Guan XY, Pan ZZ, Lan P, Xu RH and Xie D. CircLONP2 enhances colorectal carcinoma invasion and metastasis through modulating the maturation and exosomal dissemination of microRNA-17. Mol Cancer 2020; 19: 60.
[25] Wang Y, Lu JH, Wu QN, Jin Y, Wang DS, Chen YX, Liu J, Luo XJ, Meng Q, Pu HY, Wang YN, Hu PS, Liu ZX, Zeng ZL, Zhao Q, Deng R, Zhu XF, Ju HQ and Xu RH. LncRNA LINRIS stabilizes IGF2BP2 and promotes the aerobic glycolysis in colorectal cancer. Mol Cancer 2019; 18: 174.
[26] Jung G, Hernandez-Illan E, Moreira L, Balaguer F and Goel A. Epigenetics of colorectal cancer: biomarker and therapeutic potential. Nat Rev Gastroenterol Hepatol 2020; 17: 111-130.
[27] Stangeland B, Mughal AA, Grieg Z, Sandberg CJ, Joel M, Nygard S, Meling T, Murrell W, Vik Mo EO and Langmoen IA. Combined expressional analysis, bioinformatics and targeted proteomics identify new potential therapeutic targets in glioblastoma stem cells. Oncotarget 2015; 6: 26192-26215.
[28] Qiao Y, Chen J, Ma C, Liu Y, Li P, Wang Y, Hou L and Liu Z. Increased KIF15 expression predicts a poor prognosis in patients with lung adenocarcinoma. Cell Physiol Biochem 2018; 51: 1-10.
[29] Li Q, Qiu J, Yang H, Sun G, Hu Y, Zhu D, Deng Z, Wang X, Tang J and Jiang R. Kinesin family member 15 promotes cancer stem cell phenotype and malignancy via reactive oxygen species imbalance in hepatocellular carcinoma. Cancer Lett 2020; 482: 112-125.
[30] Jeong SH, Hong HS, Lee EH, Kwak JJ and Lee JY. Analysis of RAS mutation in thyroid nodular hyperplasia and follicular neoplasm in a Korean population. Endocrinol Diabetes Metab 2018; 1: e00040.
[31] Gao L, Zhang W, Zhang J, Liu J, Sun F, Liu H, Hu J, Wang X, Wang X, Su P, Chen S, Qu S, Shi B, Xiong X, Chen W, Dong X and Han B. KIF15-mediated stabilization of AR and AR-V7 contributes to enzalutamide resistance in prostate cancer. Cancer Res 2021; 81: 1026-1039.
[32] Ge W, Chen Y, Guo Y, Zhao D, Mu L, Zhang K and Zhuo W. KIF15 upregulation promotes leiomyosarcoma cell growth via promoting USP15-mediated DEK deubiquitylation. Biochem Biophys Res Commun 2021; 570: 117-124.
[33] Yang J, Peng H, Xu Y, Xie X and Hu R. SQSTM1/p62 (sequestosome 1) senses cellular ubiquitin stress through E2-mediated ubiquitination. Autophagy 2018; 14: 1072-1073.
[34] Mattiroli F and Penengo L. Histone ubiquitination: an integrative signaling platform in genome stability. Trends Genet 2021; 37: 566-581.
[35] Venkatesh D, O'Brien NA, Zandkarimi F, Tong DR, Stokes ME, Dunn DE, Kengmana ES, Aron AT, Klein AM, Csuka JM, Moon SH, Conrad M, Chang CJ, Lo DC, D'Alessandro A, Prives C and Stockwell BR. MDM2 and MDMX promote ferroptosis by PPARalpha-mediated lipid remodeling. Genes Dev 2020; 34: 526-543.

[36] Kim JY, Lee R, Xiao G, Forbes D and Bargonetti J. MDM2-C functions as an E3 ubiquitin ligase. Cancer Manag Res 2020; 12: 7715-7724.
[37] Maffeis V, Nicole L and Cappellesso R. RAS, cellular plasticity, and tumor budding in colorectal cancer. Front Oncol 2019; 9: 1255.
[38] Alcantara KMM, Malapit JRP, Yu RTD, Garrido JAMG, Rigor JPT, Angeles AKJ, Cutiongco-de la Paz EM and Garcia RL. Non-redundant and overlapping oncogenic readouts of non-canonical and novel colorectal cancer KRAS and NRAS mutants. Cells 2019; 8: 1557.

Supplementary Table 1. Target sequences and shRNA sequences used for gene knockdown

Gene symbol	Target sequence		shRNA sequences (5'-3')
KIF15	GCTGAAGTGAAGAGGCTCAAA	Pbr-00141a	ccggGCTGAAGTGAAGAGGCTCAAActcgagTTTGAGCCTCTTCACTTCAGCtttttg
		Pbr-00141b	aattcaaaaaGCTGAAGTGAAGAGGCTCAAActcgagTTTGAGCCTCTTCACTTCAGC
KIF15	AGGCAGCTAGAATTGGAATCA	Pbr-13016a	ccggAGGCAGCTAGAATTGGAATCActcgagTGATTCCAATTCTAGCTGCCTtttttg
		Pbr-13016b	aattcaaaaaAGGCAGCTAGAATTGGAATCActcgagTGATTCCAATTCTAGCTGCCT
KIF15	AAGCTCAGAAAGAGCCATGTT	Pbr-13017a	ccggAAGCTCAGAAAGAGCCATGTTctcgagAACATGGCTCTTTCTGAGCTTTTTTTg
		Pbr-13017b	aattcaaaaaAAGCTCAGAAAGAGCCATGTTctcgagAACATGGCTCTTTCTGAGCTT
NRAS	GACAAGAAGAGTACAGTGCCA	Pbr-10255a	ccggGACAAGAAGAGTACAGTGCCActcgagTGGCACTGTACTCTTCTTGTCTTTTTg
		Pbr-10255b	aattcaaaaaGACAAGAAGAGTACAGTGCCActcgagTGGCACTGTACTCTTCTTGTC
NRAS	ACCTATGGTGCTAGTGGGAAA	Pbr-10256a	ccggACCTATGGTGCTAGTGGGAAActcgagTTTCCCACTAGCACCATAGGTTTTTTg
		Pbr-10256b	aattcaaaaaACCTATGGTGCTAGTGGGAAActcgagTTTCCCACTAGCACCATAGGT
NRAS	CTGGCCAAGAGTTACGGGATT	Pbr-10257a	ccggCTGGCCAAGAGTTACGGGATTctcgagAATCCCGTAACTCTTGGCCAGTTTTTg
		Pbr-10257b	aattcaaaaaCTGGCCAAGAGTTACGGGATTctcgagAATCCCGTAACTCTTGGCCAG

Supplementary Table 2. Primers used in qPCR

Gene	Forward primer sequence (5'-3')	Reverse primer sequence (5'-3')
KIF15	CTCTCACAGTTGAATGTCCTTG	CTCCTTGTCAGCAGAATGAAG
NRAS	AAACCTCAGCCAAGACCAGA	AACCCTGAGTCCCATCATCAC
GAPDH	TGACTTCAACAGCGACACCCA	CACCCTGTTGCTGTAGCCAAA

Supplementary Table 3. Antibodies used in western blotting and IHC

Primary antibodies in WB and IP	Dilution in WB	Source species	Company	Catalog No.
KIF15	1:1000	Rabbit	Fine test	FNab04551
ELK1	1:500	Rabbit	Abcam	ab131465
p-ELK1	1:500	Rabbit	Abcam	ab28818
ERK1/2	1:1000	Rabbit	Abcam	ab17942
p-ERK1/2	1:1000	Rabbit	Abcam	ab201015
Ras	1:2000	Rabbit	Abcam	ab52939
NRAS	1:1000	Rabbit	Abcam	ab154291
Ubiquitin	1:1000	Mouse	Santa Cruz	Sc-47721
MDM2	1:2000	Rabbit	Proteintech	27883-1-AP
GAPDH	1:3000	Rabbit	Bioworld	AP0063
Primary antibodies in IHC	**Dilution in IHC**	**Source species**	**Company**	**Catalog No.**
KIF15	1:100	Rabbit	Fine test	FNab04551
NRAS	1:100	Rabbit	Bioss	bs-1146R
Secondary antibody	**Dilution**		**Company**	**Catalog No.**
HRP Goat Anti-Rabbit IgG (WB and IP)	1:3000		Beyotime	A0208
HRP Goat Anti-Mouse IgG (WB and IP)	1:3000		Beyotime	A0216
HRP Goat Anti-Rabbit IgG (IHC)	1:200		Abcam	Ab111909

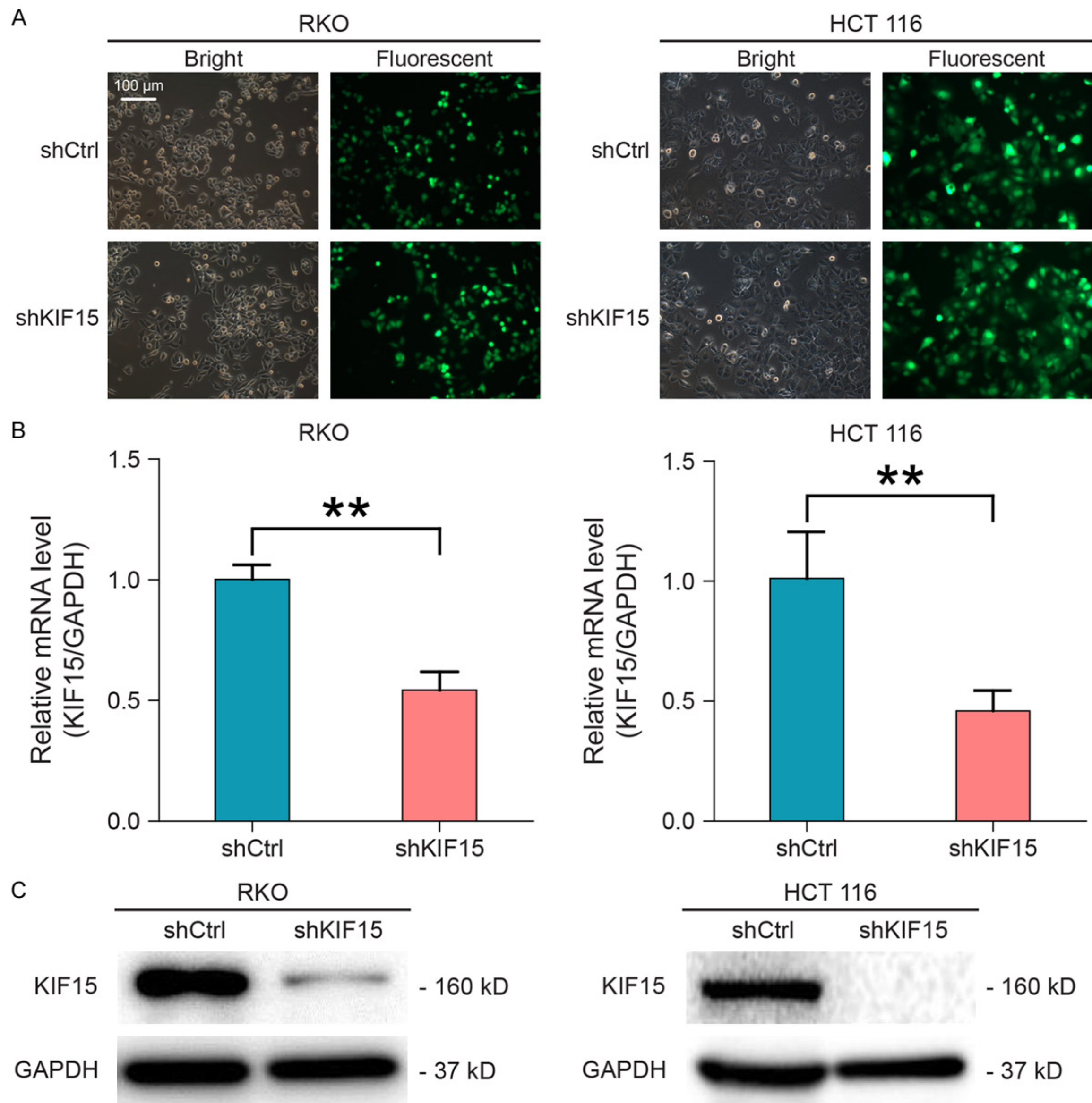

Supplementary Figure 1. CRC cell lines with KIF15 knockdown were constructed successfully *in vitro*. A. The infection efficiencies of lentivirus expression vector were observed under the fluorescence microscope. Magnification times: 200 ×. B. The levels of KIF15 mRNA were quantified by qPCR to evaluate the knockdown efficiency of shKIF15. Statistical analysis of the detection results between the two groups was conducted using t test. C. KIF15 protein expressions in CRC cell lines after shRNA infection were detected by WB. ShCtrl: CRC cells infected with negative control shRNA lentivirus; shKIF15: CRC cells infected with KIF15-shRNA lentivirus. $^{**}P < 0.01$.

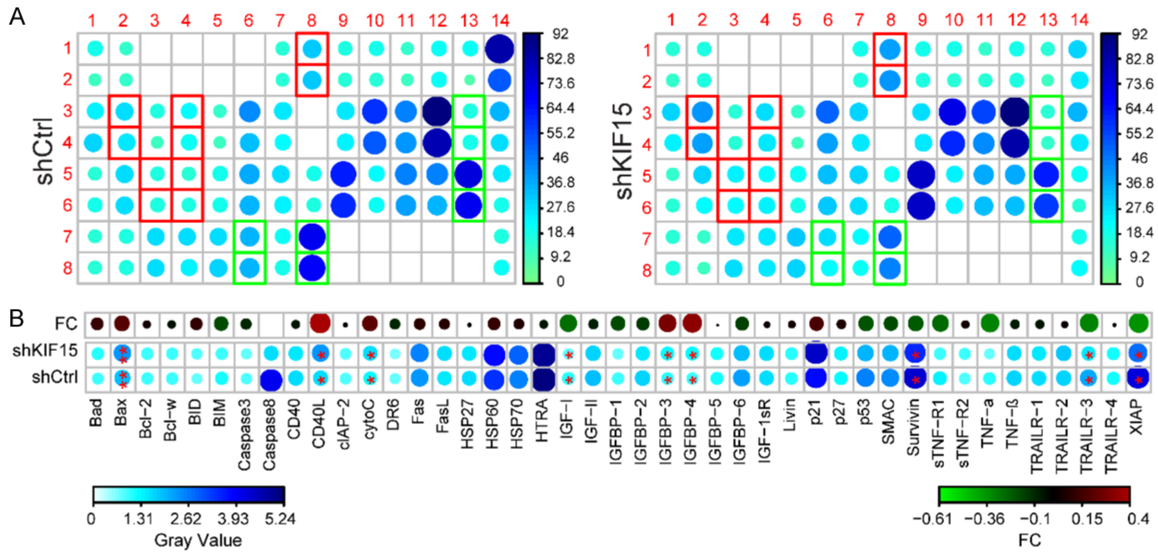

Supplementary Figure 2. The possible mechanism of KIF15 knockdown in promoting apoptosis was investigated by Human Apoptosis Antibody Array. A. After shKIF15 infection, the levels of proteins in Human Apoptosis Antibody Array were measured. Red box represented that the protein was significantly upregulated; green box represented that the protein was significantly downregulated. B. Gray value and fold change of gray value were represented in different colors and compared between the shCtrl and shKIF15 groups. ShCtrl: CRC cells infected with negative control shRNA lentivirus; shKIF15: CRC cells infected with KIF15-shRNA lentivirus. *$P < 0.05$, **$P < 0.01$.

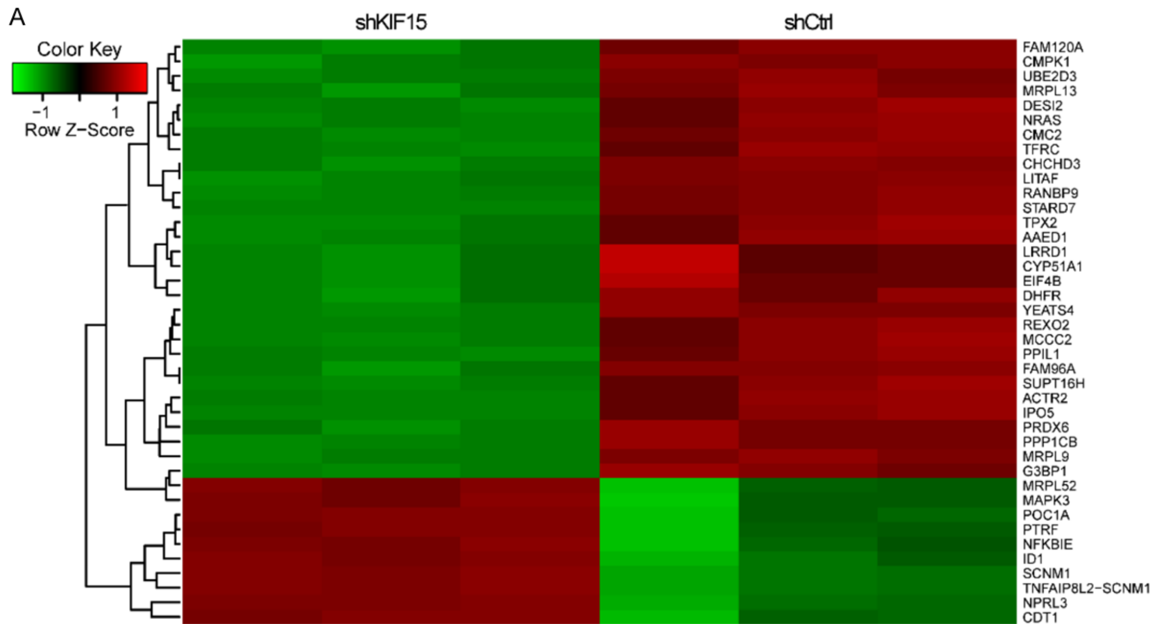

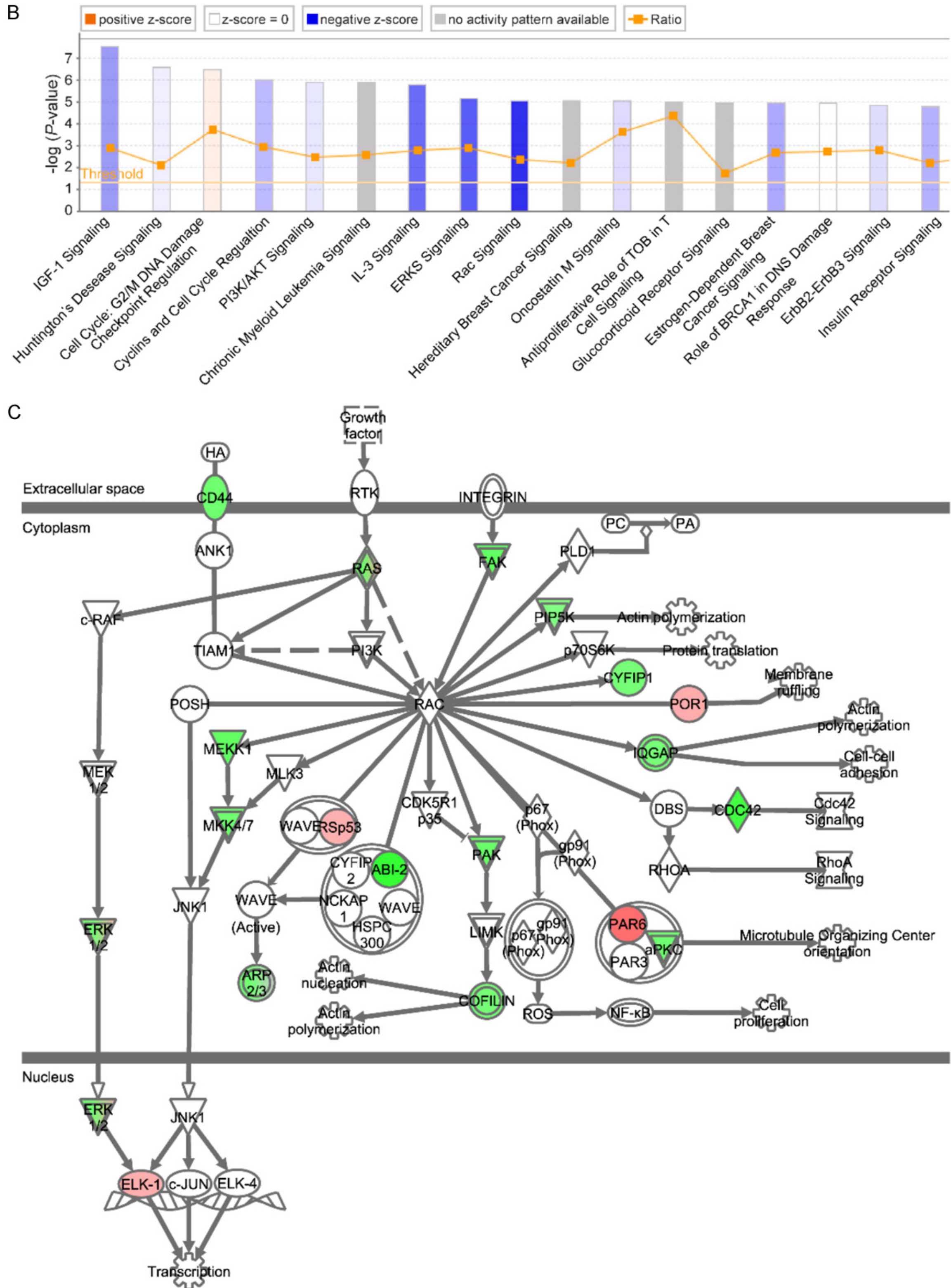

Supplementary Figure 3. The downstream mechanism of KIF15 in CRC was explored by IPA. A. Differential expression analysis was performed, so as to screen out genes with dysregulated expression in the CRC cells after KIF15 knockdown. B. The histogram of the signaling pathway showed the enrichment of differentially expressed genes in the classical signaling pathways. Orange represented the activated pathways (Z-score > 0), while blue represented the inhibited pathways (Z-score < 0). Ratio was the ratio of the number of differential genes in this pathway to the number of all genes contained in this pathway. C. The regulatory mechanism diagram of Rac signaling pathway visually showed the expression and interaction of genes in this pathway. Red meant that the gene was significantly

upregulated in differential analysis; green indicated that the gene significantly downregulated in differential analysis; white represented the molecule contained in the pathway, but it was not included in the list of differential genes. ShCtrl: CRC cells infected with negative control shRNA lentivirus; shKIF15: CRC cells infected with KIF15-shRNA lentivirus.

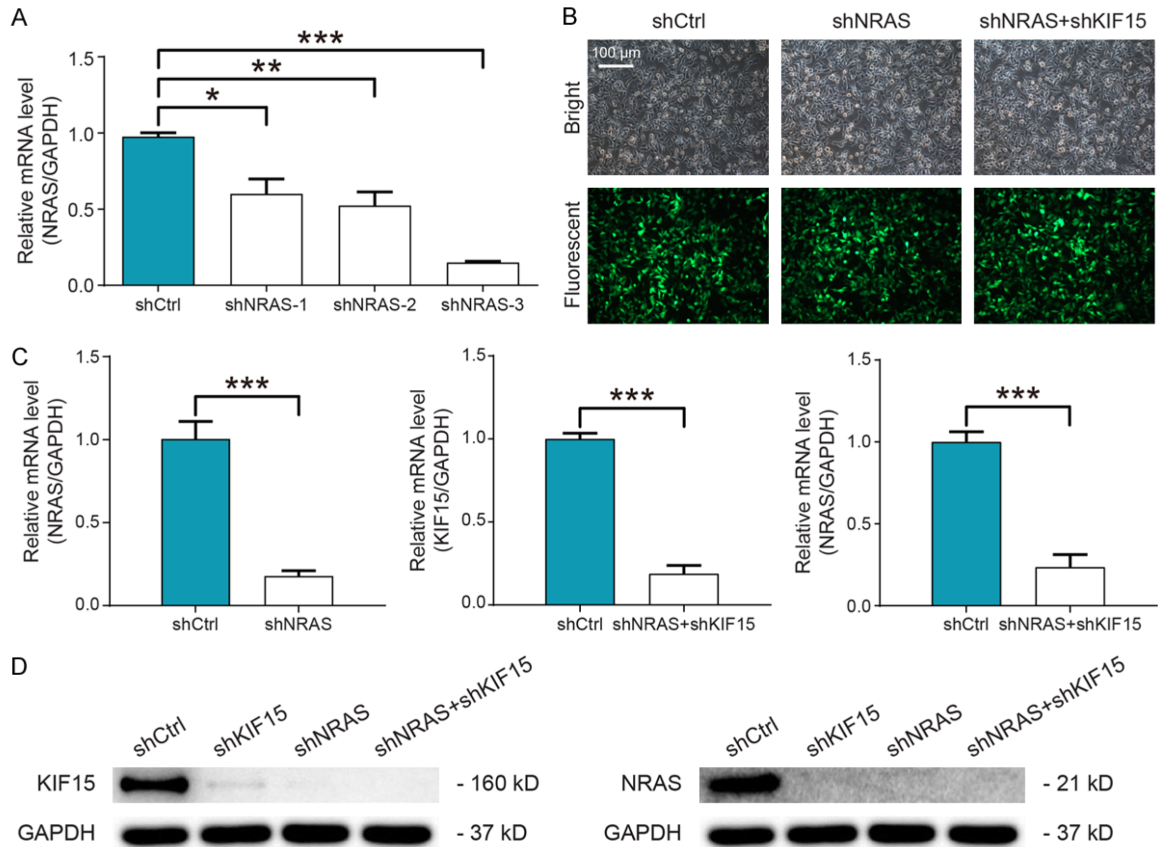

Supplementary Figure 4. CRC cell lines with NRAS knockdown as well as both NRAS and KIF15 knockdown were constructed successfully *in vitro*. A. qPCR was employed to detect the levels of NRAS mRNA in the CRC cells after infecting with different shNRAS. Statistical analysis of the detection results between the two groups was conducted using t test. B. The infection efficiencies of lentivirus expression vector were observed under the fluorescence microscope. Magnification times: 200 ×. C. The levels of NRAS and KIF15 mRNA were quantified by qPCR to evaluate the knockdown efficiency of shNRAS and shKIF15. Statistical analysis of the detection results between the two groups was conducted using t test. D. NRAS and KIF15 protein expressions in CRC cell lines after shRNA infection were detected by WB. ShCtrl: CRC cells infected with negative control shRNA lentivirus; shNRAS: CRC cells infected with NRAS-shRNA lentivirus; shNRAS+shKIF15: CRC cells infected with NRAS- and KIF15-shRNA lentivirus. $^{*}P < 0.05$, $^{**}P < 0.01$, $^{***}P < 0.001$.

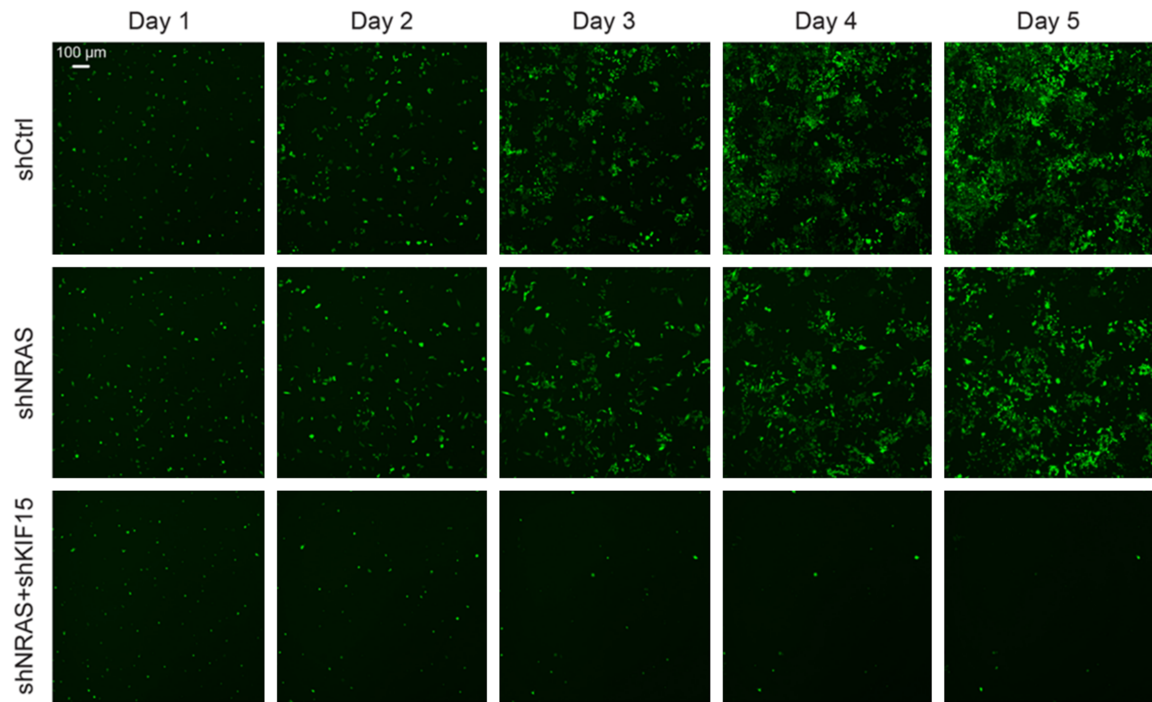

Supplementary Figure 5. Representative images of Celigo cell counting assay in shCtrl, shNRAS and shNRAS+ shKIF15 groups. Cell count was detected by Celigo for 5 consecutive days to evaluate the effects of KIF15 and NRAS on CRC cell proliferation. ShCtrl: CRC cells infected with negative control shRNA lentivirus; shNRAS: CRC cells infected with NRAS-shRNA lentivirus; shNRAS+shKIF15: CRC cells infected with NRAS- and KIF15-shRNA lentivirus.